IC/P6-46

Interaction of Ambipolar Plasma Flow with Magnetic Islands in a Quasi-Axisymmetric Stellarator

A. Reiman[1], M. Zarnstorff[1], D. Mikkelsen[1], L. Owen[2], H. Mynick[1,] S. Hudson[1], D. Monticello[1]

[1]*Princeton Plasma Physics Laboratory, Princeton, NJ 08543*
[2]*Oak Ridge National Laboratory, Oak Ridge, Tennessee*
email contact of main author: reiman@pppl.gov

Abstract. A reference equilibrium for the US National Compact Stellarator Experiment is predicted to be sufficiently close to quasi-symmetry to allow the plasma to flow in the toroidal direction with little viscous damping, yet to have sufficiently large deviations from quasi-symmetry that nonambipolarity significantly affects the physics of the shielding of resonant magnetic perturbations by plasma flow. The unperturbed velocity profile is modified by the presence of an ambipolar potential, which broadens the profile and improves the shielding near the plasma edge. In the presence of a resonant magnetic field perturbation, nonambipolar transport produces a radial current, and the resulting **jxB** force resists departures from the ambipolar velocity and enhances the shielding.

1. Introduction

Resonant magnetic perturbations pose a threat to flux surface integrity in toroidal magnetic confinement configurations. The width of the island produced by a resonant perturbation scales as the square root of the perturbation amplitude, so that even a relatively small resonant magnetic perturbation at a rational surface can produce a substantial magnetic island. Resonant perturbations can be shielded out at rational surfaces by plasma flow.[1,2] This effect is believed to play a major role in reducing the vulnerability of present day tokamaks to resonant field errors, and an understanding of the effect will be important for setting field-error tolerances for ITER. The flow shielding effect has been studied systematically in tokamak experiments where externally imposed magnetic field perturbations have been varied and their penetration threshold determined.[3,4,5]

This paper considers the flow-shielding effect in a quasi-axisymmetric stellarator. Quasi-axisymmetric stellarator configurations have drift trajectories that look like those in an axisymmetric configuration, and they allow undamped toroidal flow.[6] In the limit of perfect quasi-axisymmetry, the flow shielding effect is predicted to look like that in a tokamak having the same parameters. However, if we allow for the presence of non-quasi-symmetric ripple in the field, the radial transport is no longer intrinsically ambipolar, as it is in axisymmetric configurations. This brings in an additional radial current which modifies the physics of the flow shielding. The radial current produces a **j x B** torque that resists externally induced changes in the flow velocity and enhances the effectiveness of the shielding. It also modifies the unperturbed rotation velocity of the plasma in the absence of a resonant perturbation.

The work described in this paper focuses on a particularly interesting regime of intermediate ripple amplitude, where the deviations from quasi-symmetry are sufficiently large to substantially modify the flow-shielding effect, but where the configuration is nonetheless sufficiently close to quasi-symmetry that the flow damping in the toroidal direction can be considered to be negligibly small compared to that in the poloidal direction. A reference equilibrium for the US National Compact Stellarator Experiment (NCSX) is calculated to be in this intermediate regime[7], and the numerical calculations presented in this paper focus on that NCSX reference equilibrium. The unperturbed ambipolar velocity profile is calculated to be broader than the velocity profiles seen in tokamaks, suggesting that it will provide greater

shielding for low order rational surfaces near the plasma edge, with potential consequences for possible startup scenarios.

The three-dimensional NCSX device will have great flexibility for controlling resonant magnetic field components and investigating their interaction with plasma flow. Comparison of theoretical predictions with experimental observations on NCSX, and with tokamak experiments having comparable plasma parameters, will contribute towards the goal of being able to reliably predict field error penetration thresholds.

The NCSX, under construction at Princeton, is a quasi-axisymmetric stellarator designed to combine favorable features of advanced tokamaks with those of drift-optimized stellarators. The NCSX configuration has been designed to have good flux surfaces, incorporating several layers of defense against excessive magnetic island formation, but flow shielding could nonetheless have an impact on flexibility and on vulnerability to field errors. For the design of the NCSX, an optimization code built around the PIES three-dimensional equilibrium code was used in the coil-design process to reduce the magnitude of resonant components of the magnetic field while preserving desired engineering and physics properties. A series of calculations with the PIES code showed that this coil design process, which targeted the resonant components of the magnetic field in the NCSX reference equilibrium, also greatly reduced the island widths for a range of equilibria with varying profiles, betas, and coil currents.[8,9] The NCSX design also incorporates two sets of trim coils to provide further control over resonant magnetic fields. NCSX has also been designed to have a monotonically increasing ι (=1/q) profile to give neoclassical suppression of magnetic islands, and this is expected to further protect against magnetic island formation. Nevertheless, to the extent that the plasma flow shields out residual resonant magnetic field components at rational surfaces, it will further improve the flexibility of the NCSX device to generate a range of configurations with good flux surfaces, and it will further reduce the vulnerability of the NCSX device to field errors produced by finite tolerances in the construction and placement of the magnetic field coils.

The calculations described in this paper have been done for a reference β = 4% NCSX equilibrium whose properties are extensively discussed in a special volume of the journal Fusion Science and Technology devoted to the NCSX physics design.[10]

2. Shielding of Rational Surfaces by Plasma Flow in a Quasi-Axisymmetric Stellarator

In an ideal plasma, reconnection is prohibited and the flux surfaces cannot be broken. A surface current is induced at the rational surface that shields out resonant magnetic perturbations. In the absence of plasma flow, the presence of even a small resistivity causes the surface current to decay, and allows the resonant field to penetrate the rational surface. If flow is present at the rational surface, a localized current continues to be induced which partially shields out the resonant component of the field. If the flow is sufficiently strong, or the perturbation sufficiently weak, only a very small fraction of the resonant field penetrates the rational surface.

The induced current at the rational surface interacts with the remnant of the resonant field there to produce a $\mathbf{j} \times \mathbf{B}$ torque. This electromagnetic torque opposes the motion of the plasma at the rational surface, and acts to slow the flow. When the resonant perturbation amplitude exceeds a threshold value, the torque is large enough to locally suppress the plasma flow, allowing the resonant perturbation to fully penetrate the rational surface.

Consider the case where a small perturbation of the magnetic field is turned on in a stellarator plasma that initially has good flux surfaces. Express the unperturbed magnetic field in magnetic coordinates: $\mathbf{B}_0 = \nabla\Psi_0 \times \nabla\theta + \iota\nabla\Psi_0 \times \nabla\varphi$, where $\mathbf{B}_0$ is the unperturbed field, and Ψ_0 is an unperturbed flux function satisfying $\mathbf{B}_0\cdot\nabla\Psi_0 = 0$. Write $\mathbf{B} = \mathbf{B}_0 + \delta\mathbf{B}$, $\Psi = \Psi_0 + \delta\Psi$. To first order we get $(n - \iota m)\,\delta\Psi_{nm} = -(\delta\mathbf{B}\cdot\nabla\Psi_0 / \mathbf{B}_0\cdot\nabla\varphi)_{nm}$. The nonresonant Fourier components just introduce small ripples in the flux surfaces. If a resonant Fourier component is present (one satisfying $n = \iota m$), the flux surface is broken and a magnetic island is produced.

The response of a rotating plasma at the rational surface to an externally imposed resonant perturbation has been calculated theoretically for a variety of regimes and under a variety of assumptions.[1,11,12] These calculations have been done for either slab or cylindrical geometry. Because the local induced current is determined by the layer physics, these calculations are relevant for shaped tokamaks and for stellarators.

The electromagnetic torque exerted on the rational surface by the resonant perturbation is opposed by a viscous torque produced by the plasma flow external to the surface. The threshold for resonant field penetration is determined by the relative magnitude of the electromagnetic torque and the viscous torque. While the physics determining the magnitude of the electromagnetic torque is the same in tokamaks and stellarators, the physics determining the viscous torque is modified in a stellarator by the radial current produced by the nonambipolar transport. In the absence of a resonant perturbation, this radial current produces an ambipolar potential and a corresponding contribution to the plasma flow. When a resonant perturbation is imposed, the electromagnetic torque causes the flow velocity to deviate locally from its ambipolar value. The radial current arising from the resulting nonambipolar transport produces a **j x B** torque that opposes the electromagnetic torque and enhances the effectiveness of the shielding.

3. Ambipolar Plasma Flow in NCSX.

In this section we calculate the plasma flow velocity profile in the absence of an external resonant perturbation for our reference $\beta = 4\%$ NCSX equilibrium.

Our transport model uses a set of one-dimensional transport equations to solve for the temperature and self-consistent radial electric field, E_r, in cylindrical geometry (large aspect-ratio, circular cross-section), with an assumed density profile. The model is described in Ref. [7]. In the absence of a radial electric field, the ions are lost more rapidly than the electrons, giving a net outward current. The radial electric field, E_r, builds up until it is sufficiently large to equalize the radial flux of the ions and electrons, $j_r = 0$.

In steady-state, the ion momentum equation determines the component of the flow perpendicular to the magnetic field: $v_{i\perp} = \mathbf{E}\times\mathbf{B}/B^2 - (1/ne)\nabla p_i \times \mathbf{B}/B^2$. There is in addition a component of the flow velocity aligned with the magnetic field, $v_{\|}$, and its magnitude is determined by the relative flow damping in the poloidal and toroidal directions. As in a tokamak, the damping in the poloidal direction is strong. The configuration is sufficiently close to quasi-axisymmetry that the flow damping in the toroidal direction is small. This implies that the flow velocity in the poloidal direction can be taken to be zero to a good approximation. (The relative viscosities have been estimated using the analytic estimates of Coronado and

Talmadge.[13].) Imposing the constraint that the poloidal component of the velocity is zero, we get $v_{\|} = (B_t / B_p) v_{\perp}$.

The calculation thus far has not taken into account momentum diffusion. We have taken the poloidal velocity to be zero because of the strong poloidal damping, and we only need to consider the toroidal component of the momentum diffusion equation. We consider the momentum diffusion equation in a cylinder, where it takes the form:

$$\rho \frac{dv_z}{dt} = \frac{1}{r}\frac{d}{dr}(\mu\rho r \frac{dv_z}{dr}) + j_r B_\theta . \quad (1)$$

Here ρ is the plasma density, μ is the (anomalous) momentum diffusivity ($\mu\rho$ is the coefficient of perpendicular viscosity), and j_r is the current produced by nonambipolar radial transport. In tokamak experiments, the anomalous momentum diffusivity has been found to be approximately equal to the anomalous cross-field thermal diffusion coefficient, and we assume that that is also the case here. Stellarators often have experimentally determined thermal diffusivities that are approximately radially constant (unlike many tokamaks), and we will adopt the simple model of taking μ to be radially constant in the following.

Equation (1) differs from the momentum diffusion equation in a tokamak by the presence of the last term, which is nonzero when the flow velocity on a flux surface is forced away from its ambipolar value.

Eq. (1) must be supplemented by boundary conditions at the origin and at the edge. At the origin, regularity requires $dv_z / dr = 0$. At the plasma edge, the boundary condition is determined by the interaction with neutrals and with the scrape-off layer, which produce a momentum flow through the plasma edge equal to $-4\pi^2 aR\mu\rho dv_z / dr$, where a is the minor radius and R is the major radius. The momentum flow is equal to the total force exerted by the neutrals and scrape-off layer, which are taken to act on a small region at the plasma edge. (We will justify this approximation below.)

Near the plasma edge, momentum is transferred to the neutrals primarily through charge exchange. Ionization reactions also must be taken into account, because they serve to impart some of the momentum picked up by the neutrals back to the ions. To estimate the rate of momentum transfer to the neutrals we use the Degas code to do a Monte Carlo calculation for a model axisymmetric geometry.[14] We expect the recycling to be dominated by the inner midplane of the 60 deg. (bullet) cross section of NCSX, so we adopt this geometry.

The momentum transfer to the neutrals is localized at the plasma edge, with the average momentum transfer rate in the zone $.96 < r/a < 1$ calculated to be about seven times as large as that in the zone $.92 < r/a < .96$. The rate of momentum transfer to the neutrals can be expected to scale roughly linearly with the plasma velocity. We write this momentum transfer rate as $\nu_n v_z$, where ν_n is a coefficient to be determined. For an edge velocity of 290 km/sec, the integrated momentum transfer rate is calculated to be about 1.2 Newtons, corresponding to $\nu_n = 4 \times 10^{-6}$ kg/sec. This gives the boundary condition $a\, dv_z(a) / d\, r = -\kappa\, v_z(a)$, with $\kappa \approx 2$.

We next estimate the momentum transfer to the scrape-off layer. We consider the case where there is a toroidal rail limiter. Field lines outside the plasma edge intercept the limiter, with a connection length of $L \approx \pi R / \iota$, where $\iota \approx .6$ is the rotational transform at the plasma edge. The ion mean free path is comparable to the connection length. Particles outside the plasma edge

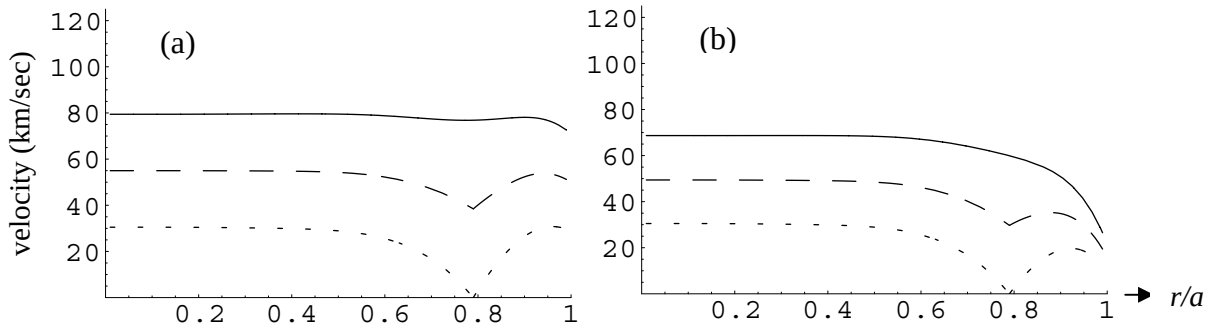

FIG. 1. Velocity profiles obtained by the numerical solution of the momentum diffusion equation, Eq. (2). Figs. (1a) and (1b) correspond to two different levels of momentum dissipation at the plasma edge: $\kappa \approx 2$ and $\kappa \approx 18$ respectively. These values of κ correspond to dissipation appropriate for neutral collisions only, and to dissipation produced by the scrape-off layer with $n_e(a) \approx 1.5 \times 10^{19}$ m^{-3}. The three curves in each figure correspond to different constraints at the rational surface. The top curve (solid) is the unconstrained solution. The middle and bottom curves correspond, respectively, to $v_s = v_{s0}/2$ *and* $v_s = 0$. *(See Section 4 for definitions of* v_s *and* v_{s0}*.)*

are lost to the limiter in a time $\tau \approx L / v_{ti}$, so that the momentum loss rate in the scrape-off layer is approximately $\rho v_z / \tau$. Combining this with momentum diffusion, and adopting a slab approximation (which is appropriate in the narrow scrape-off layer), we get $(d/dr)[\mu\rho(dv_z/dr)] = \rho v_z/\tau$. The velocity decays exponentially as a function of r in the scrape-off layer, $v_z(r) = v_z(a) \exp(-(r-a)/l)$. The density obeys a similar equation, and it too decays exponentially in the scrape-off layer. If the diffusion coefficients are equal, $l \approx 1.6\sqrt{\mu\tau}$. Momentum is dissipated in the scrape-off layer at the rate $\int_a^\infty \rho v_z/\tau \approx .6\rho(a)v_z(a)\sqrt{\mu/\tau}$. The momentum transfer rate is again of the form $\nu_n v_z$, with the scrape-off layer contribution to ν_n estimated to be roughly $0.6\rho(a)\sqrt{\mu/\tau}$. The momentum transfer to the scrape-off layer is sensitive to the value of ρ at the edge. For our assumed density profile $n_e(a) \approx 1.5 \times 10^{19}$ m^{-3}, and we calculate $\kappa \approx 18$. For smaller values of $n_e(a)$, the momentum transfer to the scrape-off layer is correspondingly smaller, with the total momentum transfer rate bounded below by the contribution of the neutrals.

Having determined the boundary conditions, we return to the solution of Eq. (1). For this purpose, we must determine the dependence of j_r on v_z. The radial current vanishes when v_z has its ambipolar value, corresponding to the ambipolar value of the electrostatic potential. We adopt a simple linear approximation for j_r, interpolating between the values for E_r=0 and for the ambipolar value of E_r. The last term in eq. (1) can then be written in the form $j_r B_\theta \approx -\alpha(r)[v_z - v0(r)]$, where v0 is the ambipolar value of v_z (i.e. the value that v_z assumes when E_r has its ambipolar value). Eq. (1) now assumes the linear form

$$\rho \frac{dv_z}{dt} = \frac{1}{r}\frac{d}{dr}(\mu\rho r \frac{dv_z}{dr}) - \alpha(r)[v_z - v0(r)] \quad (2)$$

and can be solved numerically in a straightforward manner.

The top (solid) curves in Fig. (1) show numerical solutions for the velocity profile for two different values of κ. Fig. (1a) corresponds to $\kappa \approx 2$, the lower bound on momentum dissipation due to collisions with neutrals. Fig. (1b) corresponds to $\kappa \approx 18$, the estimate for momentum dissipation in the scrape-off layer with the assumed value of $n_e(a)$.

Because the ripple magnitude increases rapidly towards the plasma edge, the flow velocity profile is broad relative to that in a tokamak. As the *q* profile evolves during tokamak startup, low order rational surfaces entering from the plasma boundary are particularly vulnerable to resonant magnetic perturbations. The broader velocity profile in NCSX will provide stronger shielding for low order rational surfaces near the plasma edge, and this will potentially impact the options available for startup scenarios.

4. Viscous Torque on Rational Surfaces

When a resonant magnetic field perturbation is imposed on a rotating plasma, the resulting electromagnetic force slows the plasma rotation at the rational surface. The electromagnetic force is balanced by a viscous force exerted by the neighboring plasma on the rational surface, which opposes the slowing of the plasma at the rational surface. As the amplitude of the external perturbation is increased, the electromagnetic force increases, and the rotation velocity of the plasma at the rational surface decreases further. The magnitude of the viscous force on the rational surface is determined by the momentum diffusion equation.

In addition to the viscous force on the rational surface, there is also a direct **j x B** torque exerted by the current that arises from the non-ambipolar transport. The total torque exerted directly by the radial current is obtained by integrating the torque density across the boundary layer at the rational surface. For the case considered here, the viscous torque is estimated to be much larger than the torque exerted directly by j_r.

We again consider the reference NCSX equilibrium whose unperturbed velocity profile we discussed in the previous section. The $\iota = 3/5$ rational surface is of particular concern because of its low order and because of its proximity to external perturbations. (It is located at $r/a \approx 0.8$.) The m=5, n=3 island proved to be the island that was the most difficult to suppress in the NCSX coil design process. We consider here the resonant mode penetration at the $\iota = 0.6$ rational surface in the presence of the ambipolar flow. Assuming that an externally generated m=5, n=3 perturbation slows the rotation of the the rational surface, we calculate the countervailing viscous force. We solve the momentum diffusion equation for this purpose.

The solution of Eq. (2) is obtained under the assumption that the electromagnetic force has slowed the rotation to a fraction of its ambipolar value. Denote the velocity at the rational surface by v_s, and the unperturbed velocity at the rational surface by v_{s0}. We consider the case where $v_s = v_{s0}/2$, and the case where $v_s = 0$. Figures (1a) and (1b) show, respectively, the corresponding solutions of Eq. (2) for $\kappa \approx 2$ and $\kappa \approx 18$. In each plot, the top curve corresponds to the solution in the absence of an electromagnetic force, the middle curve corresponds to the solution when the velocity at the $\iota = .6$ rational surface is slowed to half its ambipolar value, and the bottom curve corresponds to the solution when the rotation at the rational surface is entirely suppressed.

The viscous force exerted on the rational surface by the plasma flow is given by $4\pi^2 rR\rho\mu\left[\mathrm{dv/dr}\right]_-^+$, where $\left[\mathrm{dv/dr}\right]_-^+$ is the jump in the radial derivative of the fluid velocity across the associated boundary layer. For $\kappa \approx 2$, we calculate $a\left[\mathrm{dv/dr}\right]_-^+ \approx 274$ km/sec and 540 km/sec respectively for $v_s = v_{s0}/2$ and $v_s = 0$. For $\kappa \approx 18$ we calculate $a\left[\mathrm{dv/dr}\right]_-^+ \approx 238$ km/sec and 478 km/sec respectively. Relative to v0, the velocity on axis for the unconstrained velocity profile, we have $a\left[\mathrm{dv/dr}\right]_-^+ \approx 3.4\ v_0$ and $6.8\ v_0$ for $\kappa \approx 2$, $a\left[\mathrm{dv/dr}\right]_-^+ \approx 3.5\ v_0$ and $7.0\ v_0$ for $\kappa \approx 18$.

We compare these results with a simple tokamak model. Consider a rotating tokamak plasma driven by neutral beams with a uniform deposition profile, and take the viscosity $\mu\rho$ to be a constant. The unperturbed velocity profile is quadratic, $v = v_0 (1 - r^2 / a^2)$. Constraining $v_s = v_{s0}/2$ at $r_s/a = .8$ gives $a\left[dv/dr\right]_-^+ = -(v_0/2) (1 - r_s^2/a^2) / (r_s \ln r_s) \approx v_0$. Constraining $v_s = 0$ gives twice this value.

In a tokamak, the scale length of the velocity gradient is comparable to the minor radius, so that the jump in dv / dr is of the order of v / a. In a stellarator, the velocity gradient is determined by the magnitude of the non-ambipolar **j x B** force, so that the gradient scale length can be shorter, imparting greater stiffness to the flow velocity, and enhancing the shielding effect.

5. Resonant Mode Penetration Threshold

In mode penetration experiments on tokamaks where the amplitude of the external perturbation is gradually ramped up, it is found that the rational surface first slows to some fraction of its initial rotation frequency, and then abruptly ceases to rotate when the perturbation amplitude exceeds a threshold value. The cessation of rotation is accompanied by a complete penetration of the resonant perturbation at the rational surface. This is consistent with the predictions of theoretical calculations. The magnitudes of the viscous and electromagnetic forces are functions of v_s, and if $v_s > 0$ it must satisfy $F_{visc}(v_s) = F_{em}(v_s)$. There is predicted to be a threshold in the perturbation amplitude above which $F_{em}(v_s)$ exceeds $F_{visc}(v_s)$ for $0 \le v_s \le v_{s0}$, so that $v_s = 0$ when the perturbation amplitude exceeds this threshold.

The magnitude of F_{em} scales as the square of the resonant perturbation amplitude, with the functional dependence of $F_{em}(v_s)$ (i.e. the shape of $F_{em}(v_s)$) independent of the amplitude. Our numerical solution shows that $F_{visc}(v_s)$ is well approximated by a linear function of v_s, as it is in a tokamak, so that while its amplitude may be quite different, the functional dependence on v_s has not changed. It follows that there is again a threshold value of the resonant perturbation amplitude above which F_{em} dominates F_{visc}, and that at the threshold value v_s is the same as in the tokamak. The resonant mode penetration threshold scales as $F_{visc}^{1/2}$.

To estimate the magnitude of the flow shielding effect for magnetic islands in NCSX, we compare with a resonant mode penetration experiment on DIII-D.[4] The DIII-D reference case has been chosen to have similar parameters to those in our NCSX reference equilibrium. It has $\langle\beta\rangle \approx 3.7\%$, $\langle n_e\rangle \approx 5 \times 10^{19}$ m^{-3}, and an ellipticity $\kappa \approx 1.8$. Our reference NCSX equilibrium has $\langle\beta\rangle = 4\%$, $\langle n_e\rangle = 6 \times 10^{19}$ m^{-3}, and an average axisymmetric component of ellipticity of 1.8. The magnetic field of both the DIII-D reference shot and the NCSX reference case is 1.2 T. The rotation frequency of the rational surface in the DIII-D reference shot is about 12 kHz. For the NCSX case, the rotation frequency ranges from about 9 kHz for $\kappa \approx 2$ to about 7 kHz for $\kappa \approx 18$. DIII-D has $R \approx 1.67$ m and $R/\langle a\rangle \approx 2.1$, while NCSX has $R \approx 1.42$ m and $R/\langle a\rangle \approx 4.3$. The experimentally observed penetration threshold in the DIII-D reference case is $B_{r21} / B \approx 4\text{x}10^{-4}$.

6. Discussion

The physics determining the penetration of a resonant magnetic perturbation in a stellarator differs from that in a tokamak due to the presence of a radial current produced by nonambipolar transport. As the electromagnetic force produced by the perturbation slows the rotation at the

rational surface, the radial current driven by the resulting nonambipolar transport exerts a **j x B** force that resists departures from the ambipolar velocity and enhances the shielding effect. The unperturbed velocity profile is also modified in a stellarator. We have focused here on a particularly interesting regime, corresponding to an NCSX reference equilibrium, in which the configuration is sufficiently close to quasi-symmetry that the viscous damping in the toroidal direction is small, but the deviations from quasi-symmetry are sufficiently large to produce a substantial ambipolar flow, and a substantial modification of the flow-shielding effect. Because the ripple magnitude increases rapidly towards the plasma edge, the flow velocity profile is broad relative to that in a tokamak. The stronger shielding for low order rational surfaces near the plasma edge will have potential implications for startup scenarios.

A reference DIII-D shot with parameters similar to those of our reference NCSX equilibrium has been reported to have a penetration threshold of $B_{r21}/B \approx 4\text{x}10^{-4}$.[4] Calculations with the PIES code found that the resonant $m = 5$, $n = 3$ field component associated with an NCSX coil design algorithm that did not explicitly target resonant field error reduction was $B_{rnm}/B \approx 1.3\text{x}10^{-3}$. This is likely above the penetration threshold, even including the enhancement of the shielding due to nonambipolarity, and a further coil optimization using the PIES code to reduce the magnitude of the resonant field components was a prudent step in the coil design process. To the extent that the plasma flow shields out residual resonant magnetic field components at rational surfaces, it will further improve the flexibility of the NCSX device, and it will further reduce the vulnerability of the NCSX device to field errors.

Acknowledgment

This work was supported by DOE contract DE-AC02-76CH03073.

References

[1] R. Fitzpatrick and T.C. Hender, Phys. Fluids B **3**, 644 (1991).
[2] T. C. Hender et al, Nucl. Fusion **32**, 2091 (1992).
[3] R. J. LaHaye et al, Phys. Fluids B **4**, 2098 (1992).
[4] R. J. LaHaye et al, Nucl. Fusion **32**, 2119 (1992).
[5] R. J. Buttery et al, Nucl. Fusion **39**, 1827 (1999).
[6] J. Nuehrenberg, W. Lotz, and S. Gori, in **Theory of Fusion Plasmas**, E. Sindoni, F. Troyon and J. Vaclavik eds., SIF, Bologna, 1994.
[7] D. Mikkelsen et al, Fusion Science & Tech., accepted for publication.
[8] A. Reiman et al, Fusion Science & Tech., accepted for publication.
[9] E. A. Lazarus et al, Fusion Science & Tech. **46**, 213 (2004).
[10] Physics Design of NCSX, special issue of Fusion Science & Tech., to appear.
[11] R. Fitzpatrick, Nucl. Fusion **33**, 1049 (1993); Z. W. Ma, X. Wang, and A. Bhattacharjee, Phys. Plasmas **3**, 2427 (1996); X. Wang and A. Bhattacharjee, Phys. Plasmas **4**, 748 (1997); O. A. Hurricane, T.H. Jensen, and A. B. Hassam, Phys. Plasmas **2**, 1976 (1995); F. L. Waelbroeck, Phys. Plasmas **5**, 4040 (2003).
[12] R. Fitzpatrick, Phys. Plasmas **5**, 3325 (1998).
[13] M. Coronado and J. N. Talmadge, Phys. Fluids B **5**, 1200 (1993).
[14] P. Mioduszewski et al, Fusion Science & Tech., accepted for publication.